

Gamal A. Amhalhel, Piotr Furmański

Institute of Heat Engineering

COMPARISON BETWEEN DIFFERENT DESIGN CONCEPTS OF RECEIVERS/REACTORS FOR THERMOCHEMICAL CONVERSION OF CONCENTRATED SOLAR ENERGY

In this paper, a zero-order mathematical model based on first law analysis of the **Thermochemical Energy Conversion** (TCEC) process of concentrated solar energy have been developed. The model assumptions consider the general case for which the receiver/reactor is the direct volumetric absorption and/or indirect receiver/reactor. The thermal decomposition of a single chemical species and endothermic reversible chemical reaction is considered as the reaction system. A qualitative comparison of the model results gave a satisfactory agreement with selected experimental results. The proposed model was used to compare the general thermochemical behavior of the three general types of receivers/reactors proposed for the TCEC process operating in both continuous and in the discontinuous flow regimes. Comparison of the thermal characteristics of the TCEC process with other traditional conversion processes was also performed. Finally, conclusions were drawn to assist any further development and understanding of the TCEC process.

NOMENCLATURE

- A, B, C – the reactant species, A , the product species (B and C)
 A – area, m^2
 a, b, c – stoichiometric coefficient of the reactant species, A , the product species B and C , respectively
 \bar{c}_p – molar specific heat, $kJ/(kmol \cdot K)$
 C_j – molar concentration, $kmol/m^3$
 CR – solar energy concentration ratio
 E_a – activation energy, $kJ/kmol$
 F – molar flow rate, $kmol/s$
 \bar{h} – specific molar enthalpy, $kJ/kmol$

\bar{h}_f°	– specific molar enthalpy of formation, kJ/kmol
I	– inert material
k	– frequency factor, 1/s
m	– mass, kg
\dot{m}	– total mass flow rate, kg/s
M	– molecular mass, kg/kmol
\bar{R}	– universal gas constant, kJ/kmol
R/R	– receiver/reactor
T	– temperature, K
t	– time, s
t_r	– reference (residence) time, s
V	– volume, m ³
X	– conversion fraction (dimensionless)
y	– mass fraction

Greek symbols

α	– convective heat transfer coefficient, kW/(m ² ·K)
$\Delta \bar{C}_{P_{ABC}}$	– molar specific heat of the chemical reaction, kJ/(kmol·K)
$\Delta \bar{h}_f^\circ(T_r)$	– standard specific molar enthalpy of the chemical reaction, kJ/kmol
ε	– emissivity
ϕ	– solar flux, kW/m ²
$\rho_{w,R}^{S,L}$	– reflectivity in the short (S) and/or long (L) wavelength of the thermal radiation spectrum of the receiver/reactor; body (R) or the wall surface (w)
σ	– blackbody constant, kW/(m ² ·K ⁴)
τ_w^S	– the transmissivity of the receiver/reactor wall material in the short-wavelength of the radiation spectrum
γ	– porosity of the porous matrix (dimensionless)
ν	– stoichiometric coefficient
Θ	– dimensionless temperature
Ω	– dimensionless time

Superscripts

L	– thermal radiation in long-wave length
*	– unreacted

Subscripts

a	– ambient
c	– cavity
DR	– direct receiver/reactor

<i>e</i>	– outlet
<i>ex</i>	– exchange (e.g. between the <i>R/R</i> wall and the <i>R/R</i> body)
<i>i</i>	– entering (inlet)
<i>j</i>	– <i>j</i> -th species
<i>R</i>	– receiver/reactor body
<i>r</i>	– reference flow state condition
<i>S</i>	– surface
<i>w</i>	– receiver/reactor wall

INTRODUCTION

The thermochemical energy conversion (TCEC) process is understood as the conversion of thermal energy into reaction enthalpy (chemical potential) by an endothermal reversible chemical reaction. Thermal energy can then be potentially recovered with the inverse exothermic reaction [1, 2, 3]. Typical examples of the TCEC process are the thermal decomposition of carbonates (e.g. calcium carbonate), hydroxides (e.g. calcium hydroxide), or sulfur trioxide. The characteristic advantages of the TCEC process over the **Sensible** and/or **Phase Change** TEC processes is that the thermal energy can, theoretically, be stored for an infinite period of time and transported for a long distance, both without the need for insulation [2, 3]. The TCEC process also has disadvantages, chiefly that: product separation is usually difficult unless one of the products is a gas, reaction rates must be sufficiently rapid under practical conditions and that there must not be changes in material and cycle during the required 30 year life period [2, 3]. In general, utilization of concentrated solar energy appears promising in developing TCEC systems [2, 3]. Its utilization in the process industry as an energy source to derive chemical reaction species which have industrial importance will also reduce reliance on the conventional, natural thermal energy sources [2, 3]. This is why the subject of the TCEC process has recently received much attention [2, 3, 4, 5, 6, 7].

The objective of this work is to conduct a detailed preliminary thermodynamic analysis of the TCEC process of concentrated solar energy carried out on an energy basis. This detailed analysis should account for all the thermal energy interactions taking place during the course of the TCEC process in the receiver/reactor which may have a transparent (no wall), semi-transparent and/or opaque wall. This will enable the definition of the quantities that characterize the TCEC process of concentrated solar energy e.g. the conversion fraction and the TCEC efficiency. These quantities will assist in comparison between the three different design concepts of receivers/reactors operating in both continuous and the discontinuous flow regimes. Comparison of the thermal characteristics of the TCEC process with other **Sensible and Phase Change** TEC processes will also be discussed.

1. LITERATURE BACKGROUND

The state of the art of theoretical and technical aspects of the TCEC process of concentrated solar energy was critically reviewed by Amhalhel and Furmanski [2]. The main results of this review are summarized in brief below. It followed from this critical review that most of the studies available dealt with the feasibility and techno-economic studies of the TCEC process of concentrated solar energy [8, 9, 10, 11, 12]. These studies revealed the feasibility of concentrated solar energy to derive reversible endothermic chemical reactions and the possibility of developing TCEC storage/transport systems and thermochemical power plant [2].

The mathematical models reported in the literature refer to the steady-state one-dimensional model of the TCEC processes of **gas-based reaction systems** in the helix type, integrated cavity type and direct absorption catalytic receivers/reactors [4, 5, 6, 13, 14]. Won et al [13] modelled the thermal decomposition of sulfur trioxide as the reaction system in the helix type receiver/reactor. The integrated cavity type receiver/reactor was also modelled with carbon dioxide reforming methane with the additional water shift reaction (side reaction) as the reaction system [4, 5, 14]. Experimental studies to assist these mathematical models were also reported in [4, 5, 13, 14]. The direct volumetric absorption catalytic receiver/reactor was modelled utilizing a one-dimensional mathematical plug flow model [6]. The carbon dioxide reforming methane with the additional water shift reaction was utilized as the reaction system. The developed model was used to anticipate and predict operating conditions for the TCEC process [7]. Its results showed that mass flux must be adjusted relative to incident solar flux to provide the receiver/reactor with uniform exit conditions. The model results also revealed that most of the thermal energy exchanged was confined in a region near the front side of the receiver/reactor wall which was exposed to the solar concentrator [7]. Away from this region, both the temperature inside the receiver/reactor and the conversion fraction, were independent of the axial direction and consequently assumed an asymptotic values [7].

Solid-based reaction systems (i.e. the thermal decomposition of calcium carbonate) was also investigated experimentally using the rotary kiln and fluidized bed receivers/reactors [15, 16, 17]. The results showed that fluidized bed and rotary kiln receivers/reactors allowed continuous processing at high temperature. Proper mixing and better heat transfer characteristics made it possible to have a proper temperature distribution within the fluidized bed. Due to the material used for the construction and the configuration factor of the cavity of the rotary kiln receiver/reactor a strong thermal gradient along the axial direction of the rotary kiln was reported [15, 16, 17]. The conversion fraction, X , was calculated according to a kinetic study in a **batch isothermal reactor** heated by **electrical heating elements** [15, 16, 17]. Flamant [16, 17] defined

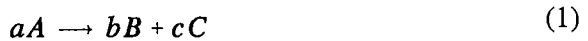
the conversion fraction as the ratio of the moles of calcium carbonate converted to calcium oxide to the moles of calcium carbonate available for disposal. The thermochemical efficiency was determined by comparing at time, t , the incident, concentrated solar energy to the thermal energy consumed (absorbed) by the chemical reaction at a conversion fraction i.e. the energy necessary to heat the calcium carbonate charge (sensible thermal energy) plus the chemical reaction enthalpy. A conversion fraction of $X = 0.3$, thermochemical efficiency of 7% and minimum energy consumption of 63 kWh/kg of lime produced were claimed. While, for the fluidized bed, the experiments results showed that total decomposition of the calcium carbonate i.e. $X = 1$ appeared after 6–8 minutes and the thermochemical efficiency was about 0.2 for partial decomposition up to $X = 0.8$ and between 0.1 and 0.15 for total decomposition [15, 16, 17]. The thermal decomposition of calcium carbonate has also been investigated experimentally using the tabular receiver/reactor [18]. Results showed that considerable conversion fractions could be obtained at higher receiver/reactor temperatures. The conversion fraction was measured by determining weight loss due to thermal decomposition at different time intervals [18]. It was also concluded that the rate of calcium carbonate decomposition by conventional heating techniques such as electric furnaces was higher than that of the concentrated solar energy source in this study [18]. This was due to the fact that decomposition of the calcium carbonate in pellet form caused the carbon dioxide gas to diffuse very slowly away from the reaction interface. This increased the decomposition temperature. Such problems can be avoided using a receiver/reactor type where temperature homogeneity and high heat transfer rates can be obtained [18].

It follows from the above studies that different types, geometries and configurations of receivers/reactors were proposed for the TCEC process [2]. The concentrated solar flux impinging on the receiver/reactor wall can also be introduced in different ways depending on the type, geometry and configuration of the receiver/reactor [2]. Different inlet and outlet locations relative to the concentrated solar flux were also possible [2]. Different base-phase chemical reaction systems were available in the literature (i.e. gas-based, solid-based and liquid-based reactions systems) which can be used for the TCEC process [2, 3]. Therefore, in order to establish a full prospective of the TCEC process of concentrated solar energy, all of these variety in the receivers/reactors, the chemical reaction systems and all the possible thermal energy exchanges taking place should be considered. The TCEC process of concentrated solar energy involves a simultaneous interaction of solar energy, mass transfer and chemical reaction. This type of problem has rarely been studied in depth and most of the experimental modeling performed so far has been performed in small scale models. Most of the governing parameters and consequently the various thermal energy exchanges, taking part in the process, were not accounted for. The quantities that characterize the TCEC process of concentrated solar energy e.g. the conversion fraction and the TCEC efficiency were also not clearly defined.

The following analysis considers the more general case of thermal decomposition of a chemical species having the general form of a single reactant, endothermic reversible chemical reaction. The mole (mass) conservation equations describe all the chemical species and the inert material which is either present or crossing the boundary of receiver/reactor and also the rate of decomposition and formation of the chemical species. The thermal energy balance comprises two energy equations, the energy equation of the receiver/reactor wall and the energy equation of the receiver/reactor body. This imposes no restrictions on what type of the base-phase reaction system should be considered and consequently on the type of the receiver/reactor employed.

2. THE MATHEMATICAL MODEL

The model analysis considers the following form of a single reactant endothermic reversible chemical reaction:



The reaction system expression is put in a more general form rather than being more particular by considering a specific form or a certain individual base-phase reaction system. Therefore, the base-phase of the reaction system, A , can be solid or gas. This will enable the study of any reaction system which has the above form, like the thermal decomposition of carbonates (e.g. calcium carbonate), hydroxides (e.g. calcium hydroxide) and sulfur trioxide which are widely studied in the literature [2].

The model consists of the receiver/reactor body and the receiver/reactor wall which may be transparent (no wall), semi-transparent or opaque. The receiver/reactor body initially consists of a solid matrix and is filled with a known mass of the reactant species A . The purpose of introducing the solid matrix is to provide support for the catalyst used, to absorb the thermal radiation volumetrically and to distribute thermal energy more evenly inside the receiver/reactor. The known total mass flow rates of the reactant species, A , and the inert species, I , are fed into the receiver/reactor system at a uniform constant temperature. At the same time the receiver/reactor is exposed to a constant concentrated solar flux. The purpose of introducing the inert species, I , is due to its role in sweeping off the product gases (e.g. in the case of a solid based reaction) and also to enable the distribution of heat more evenly inside the receiver/reactor. Initially the receiver/reactor wall and the receiver/reactor body are all at thermal equilibrium with the ambient atmosphere. As the temperature approaches the decomposition temperature of the reactant species, A , it decomposes into chemical product species, B and C .

The following additional simplifying assumptions are also employed to develop the mathematical model [3]:

- There is neither a side reaction nor a back (reverse chemical reaction) taking place.
- The system variables (e.g. temperature, catalytic activity, concentration of the chemical species) are spatially uniform throughout the receiver/reactor volume.
- The rate of the thermal decomposition of the reactant species, A , is the first order reaction and together with the temperature dependence of the specific reaction rate constant is correlated by an Arrhenius type equation.
- The solid matrix is inert to the chemical reaction.
- The receiver/reactor has a well defined rigid boundaries which characterize a constant receiver/reactor volume.
- There is no product species (B and C), present initially inside the receiver/reactor and/or in the entering total molar (mass) flow rate.
- The molar concentration of the species in the entering stream is uniform and does not vary (is constant) and equals the composition of the molar concentration of the species initially present inside the receiver/reactor.
- The receiver/reactor wall material is inert to the chemical reaction taking place.
- The specific heat of all the species is a sole function of temperature only.
- No work is done on the system (e.g. by a mixer).
- The flow inside the receiver/reactor resembles the characteristics of a plug flow.
- The difference in level for the inlet and the outlet section is small.
- The receiver/reactor body experiences a constant pressure process.
- All the species inside the receiver/reactor are in thermal equilibrium with each other and they all coexist at time $t > 0$ at the same temperature level which is the same temperature as at the exit to the receiver/reactor.
- The species present in the entering mass flow rate are all at the same temperature, T_i .
- The receiver/reactor is located in an environment of constant and uniform temperature, T_a .
- The receiver/reactor wall receives a constant and uniform rate of concentrated solar flux which is distributed uniformly all over the wall surface.
- The solar radiation is in the short-wavelength range while the radiation of the receiver/reactor body, the receiver/reactor wall and the surrounding environment is in long-wavelength range.
- The receiver/reactor wall material possesses gray-body characteristics.
- The receiver/reactor wall can be either transparent, semi-transparent or opaque to the solar radiation and exchange solar radiation from the side which is exposed to concentrated solar energy only.

2.1. MODEL EQUATIONS

The total mass balance and the separate mole balances, describing all species (A , B , C and I) which are either present or crossing the boundary of the receiver/reactor, are written as [3]:

$$\frac{dm_R}{dt} = \dot{m}_i - \dot{m}_e \quad (2)$$

$$\gamma V \frac{dC_j}{dt} = \left(\frac{y_{ji}}{M_j} \dot{m}_i \right) + v_j (C_A k e^{-E_a/\bar{R}T}) (\gamma V) - \left(\frac{y_{je}}{M_j} \dot{m}_e \right) \quad (3)$$

The term on the left hand side of Eq. (3), represents the rate of accumulation of the j -th species inside the R/R . Whereas, the first and third terms on the right hand side represent the molar flow rate of the j -th species flowing into and leaving (flowing out) the R/R , respectively. The second term, on the right hand side of Eq. (3), represents the rate of decomposition or generation of the j -th chemical species by the chemical reaction. The j -th species which occupy or cross the boundary of the R/R are: the solid matrix, the reactant species, A , the product species (B and C) and the inert species, I .

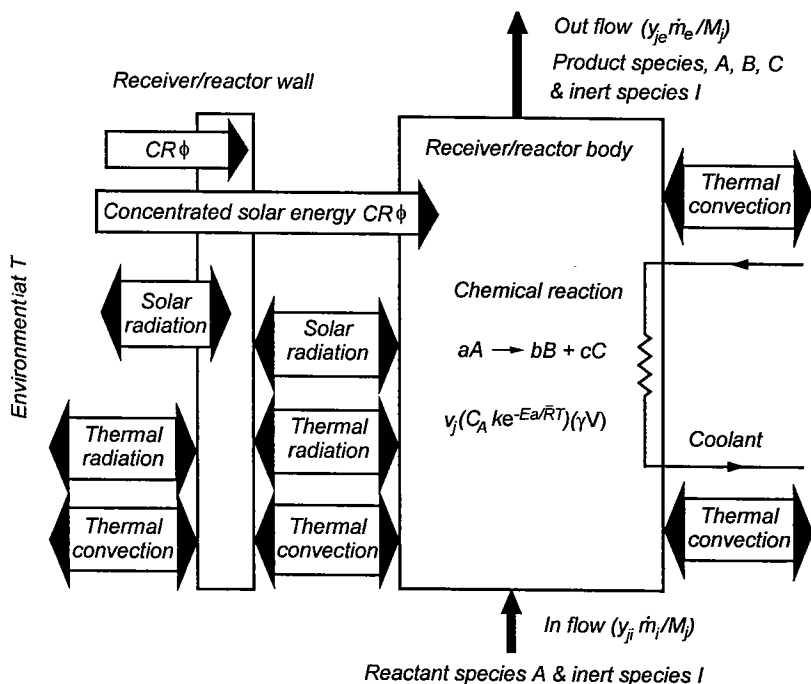


Fig. 1. Thermal energy interactions for the complete TCEC process

The receiver/reactor body equation can be also developed by applying an energy balance over the R/R body alone (Fig. 1) [3]:

$$\begin{aligned}
 \left(\sum_{j=1}^n \gamma V C_j \bar{c}_{pj} \right) \frac{dT_R}{dt} = & - \sum_{j=1}^n v_j (C_A k e^{-E_a/\bar{R}T}) \bar{h}_j - \sum_{j=1}^n F_{ji} (\bar{h}_j - \bar{h}_{ji}) + \\
 & + \frac{\tau_w^S [1 - \rho_R^S]}{(1 - \rho_w^S \rho_R^S)} A_w CR \phi + \frac{(1 - \rho_w^L)}{(1 - \rho_w^L \rho_R^L)} \epsilon_R^L \sigma A_w (T_w^A - T_R^A) + \\
 & + \alpha_{ex} A_w (T_w - T_R) - \left[\epsilon_{DR_C}^L \sigma A_{DR_C} (T_R^A - T_a^A) + \epsilon_{DR_S}^L \sigma A_{DR_S}^L (T_R^A - T_a^A) + \right. \\
 & \left. + \alpha_{DR_S} A_{DR_S} (T_R - T_a) \right]_{DR}
 \end{aligned} \quad (4)$$

The term on the left hand side of Eq. (4) represents the thermal energy accumulated within the R/R body. The first term, on the right hand side, represents the rate of thermal energy absorbed by the chemical reaction. Whereas, the second term represents the net rate of thermal energy flow across the R/R body. This term also includes the thermal energy term which accounts for the thermal energy taken by the coolant as it flows across the cooling jacket in the case of the **direct volumetric absorption receiver/reactor with no wall i.e. the rotary kiln** (see Fig. 3 in [2]). The third, fourth and fifth terms, on the right hand side, represent the thermal radiation energy in the short wavelength range intercepted by the R/R body; the thermal radiation energy exchanged in the long-wavelength range between the R/R wall and the R/R body and the thermal energy exchanged due to thermal convection between the R/R wall and the R/R body, respectively. The last three terms, inside the bracket on the right hand side of Eq. (4), are added to account for the case where the R/R wall is part of the R/R body i.e. in the case of the **direct volumetric absorption cavity type receiver/reactor with no wall, for example, the rotary kiln** (see Fig. 3 in [2]). The first two terms inside the bracket represent the thermal energy lost in the long-wavelength range of thermal radiation from the cavity opening and the outer surface of the R/R wall, respectively. Whereas the last term represents the thermal energy lost from the outer surface of the R/R to the surrounding due to convective exchange. The development of these terms were discussed in more detail in [3]. The enthalpy of the j -th species appears in Eq. (4) is defined as:

$$\bar{h}_j = \bar{h}_{jj}^o + \int_{T_r}^T \bar{c}_{pj} dT \quad (5)$$

The receiver/reactor wall equation can be developed by applying the energy balance over the R/R wall alone (Fig. 1) [3]:

$$\begin{aligned}
V_w C_w \bar{c}_{pw} \frac{dT_w}{dt} = & \left(\frac{[1 - \tau_w^S - \rho_w^S] + \rho_R^S [\tau_w^S (1 - \tau_w^S) - \rho_w^S (1 - \rho_w^S)]}{(1 - \rho_w^S \rho_R^S)} \right) A_w CR\phi + \\
& - \frac{(1 - \rho_R^L)}{(1 - \rho_w^L \rho_R^L)} \varepsilon_w^L \sigma A_w (T_w^4 - T_R^4) - \varepsilon_w^L \sigma A_w (T_w^4 - T_a^4) + \\
& - \alpha_{ex} A_w (T_w - T_R) - \alpha_w A_w (T_w - T_a)
\end{aligned} \tag{6}$$

The term on the left hand side of Eq. (6) represents the thermal energy accumulated within the R/R wall due to the thermal inertia of the wall material. The first, second and third terms on the right hand side of Eq. (6), represent the thermal radiation energy in the short-wavelength range intercepted by the R/R wall; the thermal radiation energy exchanged in the long-wavelength range between the R/R wall and the R/R body and the thermal radiation energy in the long-wavelength range lost from the outer surface of the R/R wall to the surrounding, respectively. The fourth and fifth terms represent the thermal energy exchanged between the R/R wall and the R/R body due to convection and the thermal energy lost from the outer surface of the R/R wall to the surrounding due to convective exchange. The development of these terms were discussed in a more detail in [3].

The following quantities, characterizing the TCEC process, were deduced from solution of the governing equations:

- 1) **The mole conversion fraction:** The conversion fraction of the reactant species, A , can be defined as the total moles of the reactant species, A , decomposed to the total moles of the reactant species, A , available for disposal [3]. Consequently, the expression for the conversion fraction can be written as [3]:

$$X = \frac{(C_A^* - C_A) + \int_0^t (C_A^* - C_A) \left(\frac{\dot{m}_e}{m_R} \right) dt}{C_{AO} + \int_0^t C_{Ai} \left(\frac{\dot{m}_i}{m_i} \right) dt} \tag{7}$$

where $(C_A^* - C_A)$ is the difference between the concentration of the reactant species, A , when there is no chemical reaction taking place and the concentration of the reactant species, A , when there is the chemical reaction taking place in the system.

The first term in the numerator of Eq. (7) represents the number moles of the species, A , that reacted and remained inside the R/R while the second term the number of moles of the species, A , that reacted and was removed from the R/R by the flowing stream of species. The denominator contains the expression which gives the total number of moles of the reactant species,

A , both initially present inside the R/R , C_{AO} , and the molar concentration of the reactant species, A , entering the R/R , C_{Ai} . Consequently, the conversion fraction, X , varies from zero when there is no reaction taking place to unity for the total decomposition of the reactant species. Therefore, Eq. (7) is the general equation for the mole (mass) conversion fraction, it gives the conversion fraction as measured inside and at the outlet of the R/R operating in either the continuous or the discontinuous flow regime (i.e. the semi-batch and batch flow operations) [3].

- 2) **The thermochemical energy conversion efficiency:** The TCEC efficiency is defined as the ratio of thermal energy stored in the converted reactants species, A , as it is collected at the outlet to the receiver/reactor (i.e. the net enthalpy potential associated with the chemical reaction products) at temperature level, T_R , and time, t , to the total incident concentrated solar energy [3]. Consequently, the expression for the TCEC efficiency can be written as [3]:

$$\eta_{TCE} = \frac{\int_0^t X F_{Ai} \left[\Delta \bar{h}_f^o(T_r) + \int_{T_r}^{T_R} \Delta \bar{C}_{P_{ABC}} dT \right] dt}{\int_0^t A_w CR \phi dt} \quad (8)$$

Equation (8) gives the fraction of concentrated solar energy stored in the converted reactants species, A , as it is collected at the outlet to the receiver/reactor for the R/R operating in the continuous flow regime. For the discontinuous flow regime operation, the molar flow rate of the entering reactant species, A , F_{Ai} , must be replaced by (N_{Ao}/t_r) i.e. the ratio of the number of moles of the reactants species A (initially present inside the R/R), N_{Ao} , to the time duration for which the TCEC process is processed (i.e. the residence time, t_r).

3. MODEL VERIFICATION

The governing set of first order differential equations Eqs. ((2), (3), (4) and (5)) constitute the zero-order mathematical model of the TCEC process of concentrated solar energy. These equations were solved simultaneously using the Runge-Kutta-Merson method programmed in FORTRAN 77 software [3]. The model results were verified by comparing with selected experimental results of the TCEC process utilizing thermal decomposition of calcium carbonate as the reaction system, i.e. [16, 17]



The verification of the proposed model with selected experimental results was restricted to experimental values of temperature as the conversion factor in these experiments had not been measured. Selected experiments were carried out for:

- 1) **Rotary kiln receiver/reactor operating in the continuous flow regime** (see Fig. 3 in [2]): The reported internal diameter and the length of the rotary kiln were $r_i = 0.01$ m and $l = 0.09$ m, respectively [16, 17]. The concentrated solar flux entered through the cavity opening and impinged over the surface of the reactant species. It was assumed that the rotary kiln was a **direct volumetric absorption cavity type receiver/reactor (with no wall)** and therefore, only a single energy equation (Eq. (4)) was required to describe the TCEC process. For the particular experiment, for which the model results were compared, the receiver/reactor was initially empty then it was filled with calcium carbonate (in a powder form) for about $t^* = 20$ s, i.e., with a closed outlet [17]. As the receiver/reactor was being filled the solar concentrator was switched on [17]. The mass flow rate at a steady flow state condition was $\dot{m}_i = 7 \cdot 10^{-5}$ kg/s [16, 17]. Therefore, it was assumed, in the proposed model, that the filling of the receiver/reactor could be simulated by:

$$\frac{dm_R}{dt} = D_1 \quad (10)$$

$$\left(\frac{\dot{m}_e}{\dot{m}_r} \right) = D_2 + D_3 t \quad (11)$$

where D_1 , D_2 and D_3 are constants and which were selected to give the reported value of the mass flow of calcium carbonate at the steady state flow condition. In this case, the mean reference (**residence**) time ($t_r = 91$ s), was defined as the time needed to reach the steady state flow condition [3, 17].

It was also reported that the solar power, impinging on the reactant species after concentration, was equal to 1.5 kW [17]. Therefore, it was considered in the model that $A_w CR\phi = 1,5$ kW. Due to material selectivity, the absorptivity of the rotary kiln in the short-wavelength of solar radiation was assumed to be unity [16, 17], whereas, the average value of the effective emittance of the cavity opening in the long wave-length of thermal radiation to be $\epsilon_{DR_c}^L = 0.9$ [3]. The reference temperature was taken as 25°C (i.e. $T_r = 298$ K). This temperature was selected because the thermochemical data are frequently given for this particular base [3, 19]. Several parameters describing operation of the rotary kiln were not reported in the literature

[15, 16, 17]. Therefore, it was assumed that all the species involved in the TCEC process and the surrounding were initially at 20°C. Whereas, the temperature levels of the inlet and the outlet of the coolant were assumed to be 10°C and 90°C, respectively. This is a reasonable assumption since no pressurized system has been used for the cooling water. On the other hand, the lack of information concerning: the mass flow rate of the coolant, the specific dimensions describing the internal design construction of the insulated metallic frame and the outer cooling jacket of the rotary kiln, the exact values of the chemical reaction system kinetic parameters (i.e. the activation energy, E_a , and the frequency factor, k), made it necessary to perform several trials in order to adjust numerical results with selected experimental results. For more details of the adjustment procedure, the reader should refer to [3]. The results of the adjustment procedure have revealed that the activation energy and frequency factor that gave the closest fit (Fig. 2) were found to be $E_a \approx 223$ kJ/mol and $k = 8 \cdot 10^{10}$ 1/min, respectively [3]. It can be seen from Fig. 2 that the proposed model gives satisfactory agreement with the selected experimental results.

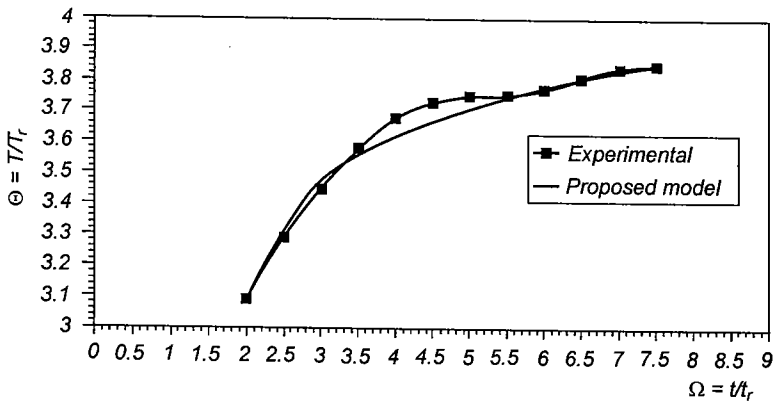


Fig. 2. Comparison of the experimental results with results of the proposed model for the rotary kiln receiver/reactor operating in the continuous flow regime

- 2) **Fluidized bed receiver/reactor operating in the discontinuous flow regime** (see Fig. 5 in [2]): Because the concentrated solar flux entered through a semi-transparent silica wall [16, 17] it was assumed that the fluidized bed was a **direct volumetric absorption receiver/reactor with a semi-transparent wall** and therefore, two energy equations (Eq. 4 and Eq. 6) described the TCEC process. In the relevant experiment a known mass of the CaCO_3 was placed inside the fluidized bed (i.e. $m_{RO} = 25 \cdot 10^{-1}$ kg) and at the same time the solar concentrator was put into operation [17]. Only the chemical product species (CO_2 in the gaseous phase) and the fluidizing gas were allowed to leave the fluidized bed. Therefore, the flow regime is consi-

dered to be a discontinuous flow regime, and the reference (**residence**) time ($t_r = 660$ s) in this case is defined as the time for which the TCEC process was processed [3].

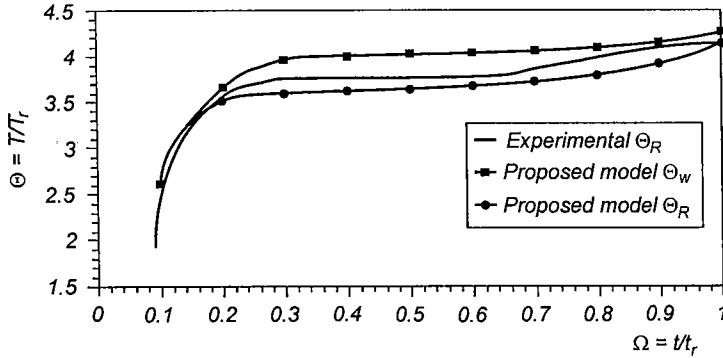


Fig. 3. Comparison of the experimental results with results of the proposed model for the fluidized bed receiver/reactor with the semi-transparent wall operating in the discontinuous flow regime

The availability of all the parameters needed to simulate the experimental work was considered. It was found that the solar power value after concentration was 1.75 kW [17]. Therefore it was assumed in the model that $A_w CR\phi = 1.75$ kW. The silica wall transmissivity was reported to be $\tau_w^S = 0.90$ [17]. Because reflectors were employed around the circumferential of the receiver/reactor wall, then the average value for reflectivity (both in the short- and long wavelength ranges of the spectrum) and the emissivity of the receiver/reactor wall were considered to be: $\rho_w^S = 0.07$, $\rho_w^L = 0.3$ and $\epsilon_w^L = 0.70$, respectively [3]. The average value for reflectivity (both in the short-wavelength and long-wavelength ranges of the spectrum) and emissivity of the receiver/reactor body were $\rho_R^S = 0.86$, $\rho_R^L = 0.40$ and $\epsilon_R^L = 0.60$, respectively, [3]. On the other hand, because the initial thermal history of the species and the receiver/reactor had not been reported it was assumed that all the species were at a temperature level of 20°C. The thermal convection heat transfer coefficient between the wall and fluidized particles depends on many factors such as: the time the particle spent in contact with the wall, the porosity of the fluidized bed and the regimes that usually characterize the flow through the fluidized beds. It was reported in the literature that the thermal convection heat transfer coefficient may lie in the range of $200 \leq \alpha_{ex} \leq 700$ W/m²K [20]. Since the exact conditions of a fluidized bed had not been reported [15, 16, 17], an assessment was made and the average value of $h_{ex} = 400$ W/m²K was selected [3]. Whereas

the average value of the thermal convective heat transfer coefficient on the outer surface of the receiver/reactor wall was assumed to be $h_w \approx 49.9 \text{ W/m}^2\text{K}$ [17]. On the other hand, the lack of information concerning: the mass flow rate of the fluidized gas, the specific length of the fluidized bed, upon which the concentrated solar energy was impinging, and the exact values of chemical reaction system kinetic parameters made it necessary to perform several trials in order to adjust the numerical results with the selected experimental results. The details of the adjustment procedure can be found in [3]. The results revealed that the activation energy and frequency factor, that gave the closest fit (Fig. 3), were $E_a \approx 240 \text{ kJ/mol}$ and $k = 8 \cdot 10^{10} \text{ 1/min}$, respectively.

4. COMPARISON BETWEEN THE THERMOCHEMICAL CHARACTERISTICS OF THE DIFFERENT DESIGN CONCEPTS OF RECEIVERS/REACTORS OPERATING IN DIFFERENT FLOW REGIMES

A comparison study of proposed model results with selected experimental results have enabled the determination of the range of the parameters to conduct the comparison study between the different design concepts of receivers/reactors [3]. For more detailed information as to the value of these parameters the reader should refer to [3]. The characteristic design feature of each type of receiver/reactor operating in each flow regime are the following:

- a) **Direct volumetric absorption cavity type receiver/reactor (with no wall).**
In this case, the main design features of the receiver/reactor were considered to be the same as those reported by Flamant for the rotary kiln [15, 16, 17].
- b) **Direct volumetric absorption receiver/reactor (with the semi-transparent wall).** In this case, the main design features of the receiver/reactor were considered to be the same as that reported by Flamant [16, 17] for a fluidized bed receiver/reactor with a semi-transparent silica wall. For continuous flow operation, the TCEC process was considered to be conducted in a tubular type receiver/reactor where the flow was considered to be a granular flow through the semi-transparent silica tube. Whereas, for operation in the discontinuous flow regime the TCEC process was considered to be conducted in a fluidized bed receiver/reactor. This will enable the demonstration of the difference between the TCEC process being conducted in the fluidized bed receiver/reactor and the tubular receiver/reactor.
- c) **Indirect receiver/reactor (with the opaque wall).** In this case the main design features and type of receiver/reactor were considered to be the same

as case b), mentioned above, except that an opaque wall (i.e. a steel wall) is utilized. It was also considered that transmissivity, average reflectivity values (both in the short- and long-wavelength range of the spectrum) and emissivity of the receiver/reactor wall were assumed to be $\tau_w^S = 0$, $\rho_w^S = 0.3$, $\rho_w^L = 0.45$ and $\epsilon_w^L = 0.55$, respectively [3]. The average reflectivity values (both in the short- and long-wavelength range of the spectrum) and emissivity of the receiver/reactor body were assumed to be $\rho_R^S = 0.0$, $\rho_R^L = 0.40$ and $\epsilon_R^L = 0.60$, respectively [3].

The flow conditions for **continuous flow operation** were assumed to be similar to those reported by Flamant [17] for the rotary kiln receiver/reactor experiment mentioned above. The difference being that, as soon as the steady state uniform flow condition is reached, the solar concentrator was switched on. The conversion fraction, X , was demonstrated as that measured at the outlet of the receiver/reactor. Whereas, for **discontinuous flow operation** the flow conditions were considered similar to those reported by Flamant [17] for the fluidized bed receiver/reactor experiment mentioned above.

For the direct absorption cavity type receiver/reactor with no wall (e.g. the rotary kiln) operating in **the continuous flow regime**, the temperature increased in a moderate trend and then assumed an asymptotic value (Fig. 4a). Whereas for receivers/reactors with a participating wall (i.e. the semi-transparent or the opaque wall), the temperature increased sharply and then assumes a constant value (Fig. 4a). This was due to the fact that the concentrated solar energy impinged over an effective area and penetrated the receiver/reactor wall through the effective height [3, 16]. It was also found that for a receiver/reactor with an opaque wall, solar power of $A_w CR\phi = 1.75$ kW resulted in a much higher temperature level which distorts the thermal energy balance of the receiver/reactor. Therefore, solar power of $A_w CR\phi = 338$ W was used. Increasing the solar power beyond this value did not improve the TCEC process, but caused the receiver/reactor wall temperature to lie outside its maximum possible practical level [3]. In spite of the fact that large values of the heat transfer coefficient ($h_{ex} \approx 400$ W/(m²K)) were used, a large temperature difference between the receiver/reactor wall and the receiver/reactor body existed for receivers/reactors with a participating wall (Fig. 4a). This temperature difference was more pronounced for receivers/reactors with the opaque wall (Fig. 4a). Consequently, only a poor conversion fraction could be achieved in a receiver/reactor with an opaque wall (Fig. 4b) i.e. $X \leq 20\%$. Whereas, a high conversion fraction can be attained in a receiver/reactor with a transparent ($X \leq 78\%$) and the semi-transparent wall ($X \leq 57\%$) (Fig. 4b). On the other hand, no substantial difference can be observed for the TCEC efficiency for these receivers/reactors (Fig. 4c).

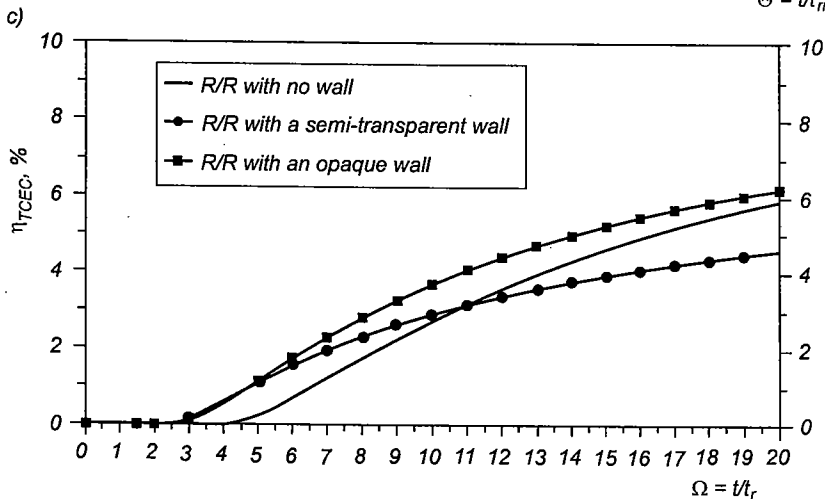
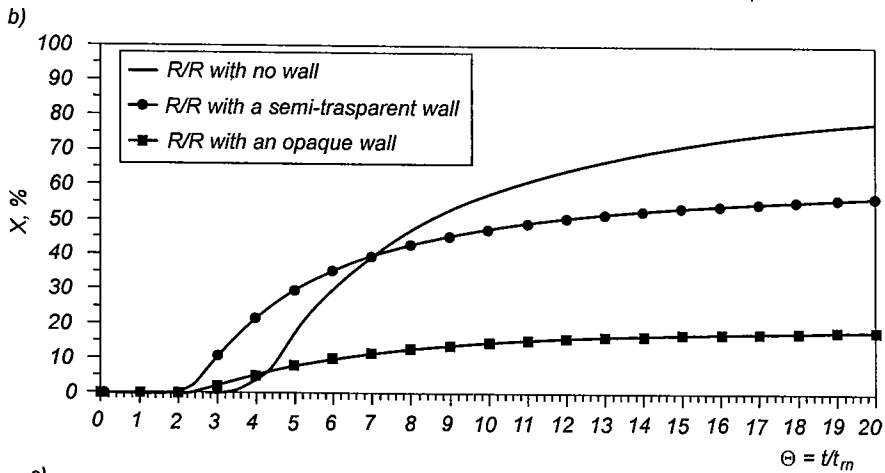
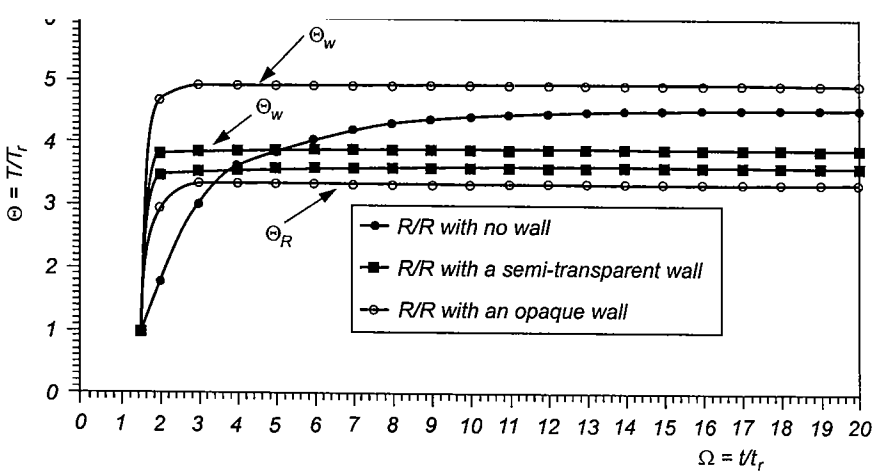


Fig. 4. a) Variation of the dimensionless temperature with the dimensionless time for the receiver/reactor operating in the continuous flow regime, b) Variation of the conversion fraction with the dimensionless time for the receiver/reactor operating in the continuous flow regime, c) Variation of the TCEC efficiency with the dimensionless time for the receiver/reactor operating in the continuous flow regime

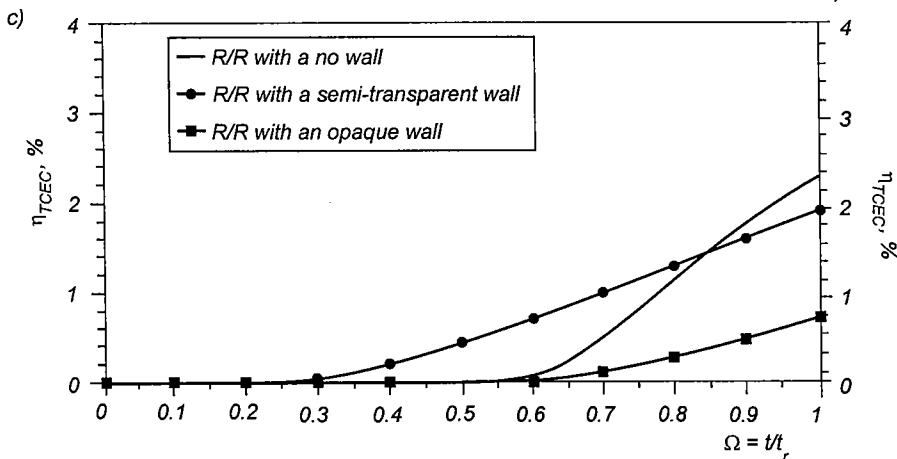
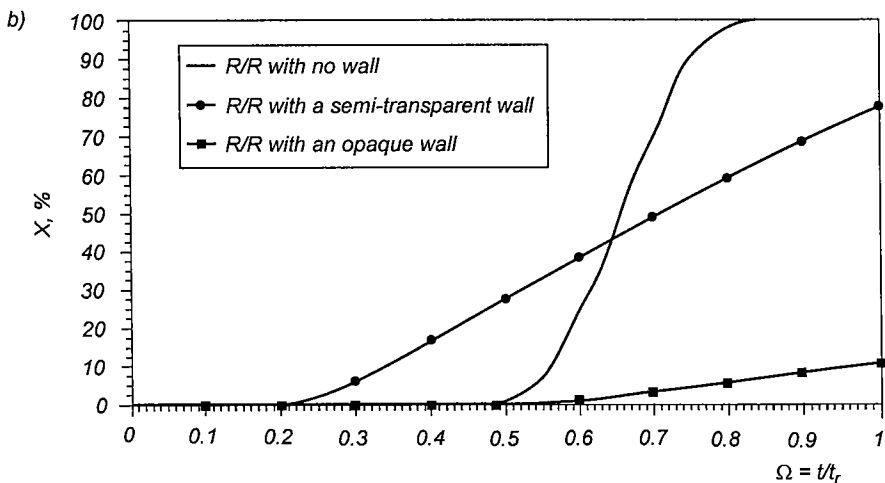
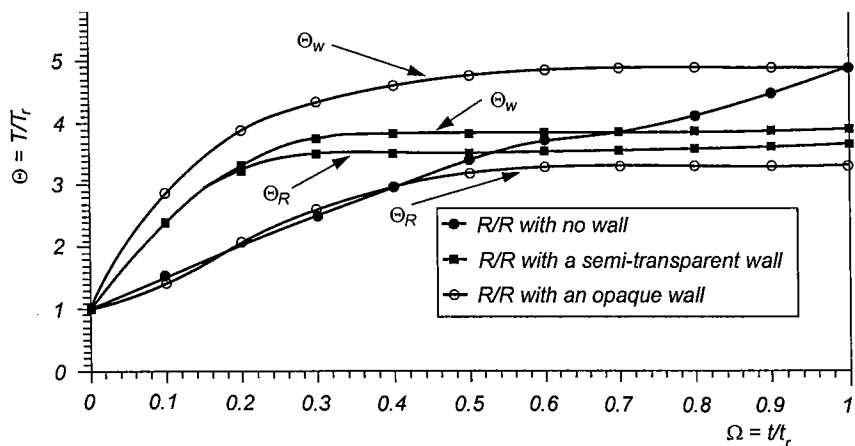


Fig. 5. a) Variation of the dimensionless temperature with the dimensionless time for the receiver/reactor operating in the discontinuous flow regime, b) Variation of the conversion fraction with the dimensionless time for the receiver/reactor operating in the discontinuous flow regime, c) Variation of the TCCEC efficiency with the dimensionless time for the receiver/reactor operating in the discontinuous flow regime

For the **discontinuous flow regime**, operating temperature increased at a slow rate and then reached a maximum value at the dimensionless time for which the TCEC process was terminated i.e. $\Omega = 1$ (Fig. 5a). It was also found that, for receivers/reactors with a participating wall a large temperature difference existed between the receiver/reactor wall and the receiver/reactor body (Fig. 5a). Consequently, the receiver/reactor with an opaque transfer wall was characterized by a very poor conversion fraction ($X \leq 12\%$) (Fig. 5b). Whereas total ($X \leq 100\%$) and partial ($X \leq 79\%$) conversion fractions can be achieved in receivers/reactors with transparent and semi-transparent walls, respectively (see Fig. 5b). These differences in conversion fraction values caused the receivers/reactors with transparent and semi-transparent walls to show higher TCEC efficiency than receivers/reactors with opaque walls (Fig. 5c).

For **both operating flow regimes**, in the receiver/reactor with a transparent wall (i.e. the rotary kiln) total conversion fractions could be achieved (Fig. 4b and Fig. 5b). This was due to the cavity effect which ensures 100% capture of concentrated solar energy. On the other hand, due to poor contact between the receiver/reactor wall and the receiver/reactor body, only partial conversion fractions could be achieved in the receiver/reactor with a semi-transparent transfer wall (see Fig. 4b and Fig. 5b). Whereas receivers/reactors with an opaque transfer wall was characterized by very poor conversion fractions (Fig. 4b and Fig. 5b). This trend was attributed to thermal energy losses experienced by the receiver/reactor wall (thermal radiation and thermal convective losses) and poor thermal contact between the receiver/reactor wall and the receiver/reactor body. The flow of the reactant species for receivers/reactors with participating walls operating in continuous flow regimes was considered to be a granular flow through tabular type receivers/reactors. This has resulted in higher conversion fraction values (Fig. 4b) than those which were obtained in fluidized bed receivers/reactors (Fig. 5b). This was because for the fluidized beds a larger value of molar flow rate of fluidized gas must be considered to account for the fluidization of CaCO_3 . This resulted further in lowering the thermal energy level of the receiver/reactor due to the cooling effect of the fluidized gas and consequently lowering conversion fraction values (Fig. 5b).

The receiver/reactors operating in the continuous flow regime showed higher TCEC efficiencies than those operating in the discontinuous flow regime (Fig. 4c and Fig. 5c). However, although a clear choice between the different design concepts of the receivers/reactors can be made on the basis of the conversion fraction, there seems to be no clear choice based on TCEC efficiency. Therefore, the selection of a particular design concept of receiver/reactor should be made based on an economic evaluation of the total cost of the TCEC process. The fact that the present results were generated for a particular set of parameters means that the TCEC efficiency, shown in Fig. 4c and Fig. 5c, does not represent the maximum possible efficiency that can be achieved in the

TCEC process. However, the problem of optimization (in depicting the maximum possible TCEC efficiency) belongs to the domain of variational calculus. The sensitivity analysis of the influence of the governing parameters showed the possibility of achieving a TCEC efficiency of 11% in the rotary kiln receiver/reactor operating in the continuous flow regime [3]. This revealed the importance of the optimization study in order to find the optimum operating and design conditions that would result in optimum TCEC efficiency of the TCEC process.

It should be noted that TCEC efficiency (in Fig. 4c and Fig. 5c) represents thermal energy converted into enthalpy potential associated with chemical reaction products, Eq. (8). If total thermal energy utilization in the TCEC process was considered i.e. the fraction of concentrated solar energy that goes into: the heating of the charge (reactant species A), the inert species, I , and the coolant (in the case of the direct volumetric absorption cavity type receiver/reactor with no wall e.g. the rotary kiln) then the overall efficiency of the TCEC process would be considerably increased [3]. The overall efficiency of the TCEC process can reach a value of 81% for the direct absorption cavity type receiver/reactor with no wall operating in **the continuous flow regime** as compared to a corresponding value of 57% for the **discontinuous flow regime operation**. Whereas, for receivers/reactors with a participating wall (i.e. a semi-transparent or the opaque wall), operating in both flow regimes, the overall efficiency of the TCEC process would be of the order of 11% and 32%, respectively. For more detailed discussion of these thermal energy utilizations the reader should refer to [3].

4.1. COMPARISON WITH OTHER THERMAL ENERGY CONVERSION PROCESSES

Different theoretical and experimental studies of Sensible and Phase Change Thermal Energy Conversion (i.e. STEC and PCTEC) processes are available in the literature which employ different types and configurations of receivers and different thermal energy sources [21, 22, 23, 24, 25, 26, 27, 28]. In these studies the first law (energy) efficiency is defined as thermal energy gained by the working fluid during time, t , to total thermal energy input during that time t . Theoretical and experimental studies of the STEC of concentrated solar energy in the fluidized bed receiver utilizing the cavity effect with alumina particles as the working medium, showed that the thermal system operating at the temperature range of $823 \leq T \leq 1188$ K with first law efficiencies of 65% could be achieved [21]. Packed and fluidized bed receivers with the semi-transparent wall had also been employed to investigate the STEC of the concentrated solar energy utilizing silicon carbide or zirconia particles as the working medium in

the temperature range of $650 \leq T \leq 1550$ K [22]. The results showed that, depending on the temperature level and the working medium, thermal efficiency lies in the range of 18.7% to 74.15% [22]. The experimental and theoretical study of the STEC of concentrated solar energy in the direct volumetric absorption receiver utilizing a porous matrix with air as a working fluid have been performed by Skocypec et al [23]. The results showed that at a temperature of 653 K, first law efficiency was 86% and decreased to a value of 69% at a temperature of 1023 K [23]. An unsteady two-dimensional analysis of a flat-plate **non-concentrating** solar collector for the STEC of solar radiation, with time varying insolation, have been performed by Onyegegbu and Morhenne [24]. Results showed that for a maximum outlet temperature of the working fluid of 350 K and for a near clear day at noon-solar time, the first law efficiency was 60% [24]. Domanski and Fellah [25] have demonstrated that under optimum charging conditions, the Sensible Thermal Energy Storage (STES) unit that employed Joulean heaters would yield the first law efficiency of 57.68%.

Bjurstrom and Carlsson [26] have employed energy analysis to evaluate both the Sensible and Latent Heat Storage units in the temperature range of $298 \leq T \leq 511$ K. Results revealed that these units were capable of having a first law efficiency of 30% [26]. An experimental study of the PCTES storage using Glauber's salt ($\text{Na}_2\text{SO}_4 \cdot 10\text{H}_2\text{O}$) in fluidized and fixed bed heat exchangers, in the temperature range of $293 \leq T \leq 313$ K has been conducted in [27]. The Glauber's salt was encapsulated in 25 mm-diameter hollow spheres and agitated when fluidized by the heat transfer medium (water). The results showed that the fluidized capsules maintained first law efficiency of 60% over 96 cycles. When encapsulated capsules of Glauber's salt were used in the rotating tube and rotating drum, results showed that the system's first law efficiency could be improved to 83% [28].

It follows from the above discussion that although the thermochemical characteristics of various types of receivers/reactors were generated for a selected set of operational parameters the TCEC efficiency was comparable in magnitude with the STEC and PCTEC processes. However, the present analysis provided means to compare the thermal characteristics of the TCEC process with the STEC and PCTEC processes based on energy analysis. The second law analysis based on the exergy concept, which considers the temperature level of the energy transfer, also provides a powerful tool for efficiency evaluation of the TCEC process. The second law of thermodynamics addresses the quality of exergy (which is not a conservative quantity) and consequently it accounts for all the irreversibilities taking place during the conversion process [25, 29]. These irreversibilities will provide a means by which the second law of the TCEC process will be defined and consequently compared with the other thermal energy conversion processes. In contemporary thermal analysis the second law analysis also assists the concept of thermoeconomics [30, 31]. These necessitate a detailed exergy analysis of the TCEC process in future work.

5. CONCLUSIONS

The present energy analysis of the TCEC process of the different design concepts of receivers/reactors allows the following conclusions to be drawn:

- a) The zero-order thermochemical model which accounts for all the possible phenomena encountered in the TCEC process of concentrated solar radiation was proposed. The model was found to give satisfactory agreement with selected experimental results. The model assisted in identifying the conversion fraction and the TCEC efficiency which characterize the TCEC process.
- b) The comparison between different design concepts of receivers/reactors, operating in both continuous and discontinuous flow regimes, indicated that for both operating flow regimes, the conversion fraction, X , lay in the range $0 \leq X \leq 100\%$ for the receivers/reactor with the transparent (no wall) and the semi-transparent wall. Whereas the opaque wall limits the range of X values to $0 \leq X \leq 20\%$. On the other hand, the continuous flow regime operation has enabled the receivers/reactors to show higher values of TCEC efficiency than that of the discontinuous flow regime operation.

The **conversion fraction** is a measure of the reactant species converted to chemical reaction products. Therefore, it offers the potential to utilize concentrated solar energy to drive industrial chemical reaction processes instead of conventional thermal energy sources (e.g. fuels). On the other hand, **TCEC efficiency** is also a measure of thermal energy converted in the reactant species that will be recovered later in the thermochemical energy recovery process utilizing the reactor/heat exchanger. Consequently, it offers the potential to store thermal energy. In general, the selection of the particular design concept of the receiver/reactor should be made based on economic evaluation of the total cost of the TCEC process.

Sensitivity analysis of the influence of the governing parameters is necessary in order to determine the maximum possible TCEC efficiency. Selected parametric study indicated the possibility of achieving a TCEC efficiency of 11% in the rotary kiln receiver/reactor operating in the continuous flow regime. This necessitates the performance of an optimization study to find the optimum operating and design conditions that would result in the optimum TCEC efficiency of the TCEC process.

- c) The thermochemical characteristics of three general types of receivers/reactors indicated that if the total thermochemical efficiency of the TCEC process is included, the overall thermal utilization of the TCEC process can be of a larger magnitude than that of the Sensible and Phase Change TEC processes.
- d) Exergy analysis is also required in order to take into account the thermal energy level of the process and to define the second law efficiency of the

- TCEC process. This will also assist in comparing the process with other Sensible and Phase Change TEC processes.
- e) Finally, modeling of the thermochemical energy recovery process is also needed in order to provide a full prospective of the utilization of the complete TCEC systems. Development of two- or three-dimensional models would also be valuable in order to scale up the particular type of the receiver/reactor for the TCEC process.

REFERENCES

- [1] Amhalhel G.A., Furmański P.: Problems of modeling flow and heat transfer in porous media. Bulletin of the Institute of Heat Engineering, Warsaw University of Technology, **85**, 1997, pp. 55–88.
- [2] Amhalhel G.A., Furmański P.: Theoretical and technical aspects of thermochemical energy conversion of concentrated solar energy. Bulletin of the Institute of Heat Engineering, Warsaw University of Technology, **89/90**, 2004, pp. 25–58.
- [3] Amhalhel G.: Thermodynamic analysis of thermochemical energy conversion of concentrated solar radiation. Ph. D. Thesis, Warsaw University of Technology, Faculty of Power and Aeronautical Engineering, 1998.
- [4] Meirovitch E.A. Segal, Levy M.: Theoretical modeling of a directly heated solar-driven chemical reactor. Solar Energy, **45**, 1990, no. 3, pp. 139–148.
- [5] Meirovitch E.: Distinctive properties of tubular solar chemical reactors. Trans. ASME J. Solar Energy Eng., **133**, 1991, pp. 188–193.
- [6] Hogan Jr. R.E., Skocypec R.D.: Analysis of catalytically enhanced solar absorption chemical reactors: Part I – Basic concepts and numerical model description. Trans. ASME, J. Solar Energy Eng., **114**, 1992, pp. 106–111.
- [7] Skocypec R.D., Hogan Jr. R.E.: Analysis of catalytically enhanced solar absorption chemical reactors: Part II – Predicted characteristics of a 100 kW reactor. Trans. ASME, J. Solar Energy Eng., **114**, 1992, pp. 112–118.
- [8] Chubb T.A.: Analysis of gas dissociation solar thermal power system. Solar Energy, **17**, 1975, pp. 129–136.
- [9] Chubb T.A., Nemecek J.J., Simmons D.E.: Application of chemical engineering to large scale solar energy. Solar Energy, **20**, 1978, pp. 219–224.
- [10] Fish J.D., Hawin D.C.: Closed loop thermochemical energy transport based on CO₂ reforming of methane: balancing the reaction system. Trans. ASME, J. Solar Energy Eng., **109**, 1987, pp. 215–220.
- [11] Prengle Jr. H.W., Sun C.H.: Operational chemical storage cycles for utilization of solar energy to produce heat or electric power. Solar energy, **18**, 1976, pp. 561–567.
- [12] Williams O.M.: Thermochemical energy transport costs for a distributed solar power plant. Solar Energy, **20**, 1978, pp. 333–342.
- [13] Won Y.S, Voecks G.E., McCrary J.H.: Experimental and theoretical study of a solar thermochemical receiver module. Solar Energy, **37**, 1986, no. 2, pp. 109–118.

- [14] Levy M.R., Levitan E., Meirovitch A., Segal H., Rosin, Rubin R.: Chemical reactions in a solar furnace 2: Direct heating of a vertical reactor in an insulated receiver. Experiments and computer simulations. *Solar Energy*, **48**, 1992, pp. 395–402.
- [15] Bdie J.M., Bonet B., Faure M., Flamant G.: Decarbonation of calcite and phosphate rock in solar chemical reactors, *Chem. Eng. Sci.*, **35**, 1980, pp. 413–420.
- [16] Flamant G.: Experimental aspects of the thermochemical conversion of solar energy; decarbonation of CaCO_3 . *Solar Energy*, **24**, 1980, pp. 385–395.
- [17] Flamant G.: *Thermochimie solaire: Etude de procedes. Application a la decarbonatation de la calcite.* These de Docteur Ingenieure, Universite Paul Sabatier, Toulouse 1978.
- [18] Salman O.A., Khraishi N.: Thermal decomposition of limestone and gypsum by solar energy. *Solar Energy*, **41**, 1988, no. 4, pp. 305–308.
- [19] Szarawara J.: *Thermodynamika Chemiczna.* Wydawnictwa Naukowo Techniczne, 2nd. ed. Warszawa 1985.
- [20] Flamant G., Menigault T.: Combined wall to fluidized bed heat transfer: Bubbles and emulsion contributions at high temperature. *Int. J. Heat & Mass Transfer*, **30**, 1987, no. 9, pp. 1803–1812.
- [21] Flamant G., Gauthier D., Boudhari C., Flitris Y.: A 50 kW Fluidized bed high temperature solar receiver: Heat transfer analysis. *Trans. ASME, J. Solar Energy Engg.*, **110**, 1988, pp. 313–320.
- [22] Flamant G., Olalde G.: High temperature solar gas heating comparison between packed and fluidized bed receivers. *Solar Energy*, **31**, 1983, no. 5, pp. 463–471.
- [23] Skocypec R.D., Boehm R.F., Chavez J.M.: Heat transfer modeling of the IEA/SSPS volumetric receiver. *ASME J., Solar Energy Engg.*, **111**, 1989, pp. 138a–143.
- [24] Onyegegbu S.O., Morhenne J.: Transient multidimensional second law analysis of time-varying insolation with diffuse component. *Solar Energy*, **50**, 1993, no. 1, pp. 85–95.
- [25] Domański R., Giurma Fellah: Exergy as a tool for designing and operating thermal storage systems. *Bulletin of Institute of Heat Engineering, Warsaw University of Technology*, **81**, 1995, pp. 23–45.
- [26] Bjurström H., Bo Carlsson: An exergy analysis of sensible and latent heat storage. *Heat Recovery systems*, **5**, 1985, no. 3, pp. 233–250.
- [27] Sozen Z.Z., Grace J.R., Kenneth L.P.: Thermal energy storage by agitated capsules of phase change material. 1: Pilot scale experiments. *Ind. Eng. Chem. Res.*, **27**, 1988, pp. 679–684.
- [28] Sozen Z.Z., Grace J.R., Kenneth L.P.: Thermal energy storage by agitated capsules of phase change material. 2: Cases of efficiency loss. *Ind. Eng. Chem. Res.*, **27**, 1988, pp. 684–691.
- [29] Szargut J.: International progress in second law analysis. *Energy*, **5**, 1980, pp. 709–718.
- [30] Domański R., Fellah G.: Thermoeconomic analysis of sensible heat thermal energy storage systems. *Applied Thermal Engineering*, **18**, 1998, no. 8, pp. 693–704.
- [31] Fellah G.: Exergy analysis for selected thermal energy storage units. Ph. D. Thesis, Warsaw University of Technology, Faculty of Power and Aeronautical Engineering, 1996.

PORÓWNANIE RÓŻNYCH UKŁADÓW ODBIORNIK PROMIENIOWANIA/REAKTOR STANOWIĄCYCH ELEMENTY UKŁADÓW DO TERMOCHEMICZNEJ KONWERSJI ENERGII SKONCENTROWANEGO PROMIENIOWANIA SŁONECZNEGO

Streszczenie

W artykule zaproponowano zerowymiarowy model układu odbiornik promieniowania/reaktor chemiczny umożliwiający analizę energetyczną termochemicznej konwersji energii (TCEC) promieniowania słonecznego. Model ten opisuje ogólny przypadek, gdy pochłanianie promieniowania słonecznego odbywa się na powierzchni lub w objętości odbiornika/reaktora. W reaktorze zachodzi endotermiczna, odwracalna reakcja chemiczna związana z rozkładem pojedynczej substancji. Jakościowe porównanie wyników otrzymanych z modelu z wynikami wybranych badań doświadczalnych, zamieszczonych w literaturze, dało zadowalający rezultat. Następnie wykorzystano opracowany model do analizy porównawczej zachowania trzech typów układu odbiornik promieniowania/reaktor zaproponowanych do realizacji procesu TCEC i pracujących przy ciągłym przepływie czynnika roboczego przez reaktor oraz przy braku przepływu czynnika. Dokonano porównania charakterystyk cieplnych procesu TCEC z innymi klasycznymi procesami konwersji energii promieniowania słonecznego. Pracę zakończono wnioskami dotyczącymi dalszego rozwoju i rozumienia procesu termochemicznej konwersji energii promieniowania słonecznego.